arXiv:1202.0947v2 [cond-mat.str-el] 26 Mar 2012

# Entanglement and boundary theories of Resonating Valence Bond wavefunctions

Didier Poilblanc,[1] Norbert Schuch,[2,3] David Pérez-García,[4] and J. Ignacio Cirac[5]
[1]*Laboratoire de Physique Théorique, C.N.R.S. and Université de Toulouse, 31062 Toulouse, France*
[2]*Institute for Quantum Information, California Institute of Technology, MC 305-16, Pasadena CA 91125, U.S.A.*
[3]*Institut für Quanteninformation, RWTH Aachen, D-52056 Aachen, Germany*
[4]*Department of Mathematical Analysis, Faculty of Mathematics, UCM, Spain*
[5]*Max-Planck-Institut für Quantenoptik, Hans-Kopfermann-Str. 1, D-85748 Garching, Germany*

We investigate the relations between bulk and boundary properties of short-range resonating valence bond wave functions using Projected Entangled Pair States. We show that, for a bipartition, the boundary Hamiltonian defined on the edge can be written as a product of a highly non-local projector, which fundamentally depends upon boundary conditions, with an emergent (local) one-dimensional (superfluid) t–J Hamiltonian, which arises due to the symmetry properties of the auxiliary spins at the edge. This multiplicative structure, a consequence of the disconnected topological sectors in the space of dimer lattice coverings, is then characteristic of the topological nature of the states. For systems with open boundary conditions, it is shown that the entanglement spectrum, which reflects the properties of the (gapped or gapless) edge modes, is a subset of the spectrum of the local Hamiltonian, also explaining the origin of the topological entanglement entropy. We propose to use these features to probe topological phases in microscopic Hamiltonians.

PACS numbers: 71.10.-w,75.10.Kt,03.67.-a,03.65.Ud

Conventional ordering in condensed matter systems is traditionally associated to symmetry-breaking and to the existence of a local order parameter (Landau theory). Topologically ordered phases of matter [1] offer completely new classes of systems for which the ground state (GS) degeneracy depends on topology (disc, cylinder, torus, etc...). The (short-range singlet) Resonating Valence Bond (RVB) wavefunction proposed by Anderson [2] as the parent Mott insulator of high-temperature superconductors is a celebrated example. Such topological phases carry emerging fractionalized excitations and raise growing attention due to their potential to realize fault-tolerant setups for quantum computing. [3]

Interest for topological liquids in quantum antiferromagnets [4] and in related microscopic models [5–8] has also triggered the search for novel theoretical tools capable of detecting topological order, in particular entanglement measures used in quantum information. A common setup consists of dividing the system into two regions (named A and B) and compute the reduced density matrix (RDM) in the GS of e.g. the A subsystem. The entanglement entropy (EE), defined as the Von Neumann entropy of the RDM $S_{\rm VN} = -\rho_A \ln \rho_A$, contains an extensive term – proportional to the length of the boundary (area law) – and a universal sub-leading constant, the topological EE. Specific disc-like setups [9] or cylindrical geometries can be used to extract the topological EE.

In fact, $-\ln \rho_A$ can be seen as a (dimensionless) Hamiltonian $H_b$, a key conceptual object. First, its spectrum, the so-called entanglement spectrum (ES), has been conjectured to show a one-to-one correspondence with the spectrum of edge states. This remarkable property was first established in fractional quantum Hall states [10] and, then, in quantum spin systems [11]. Furthermore, Projected Engangled Pair States (PEPS) [12] offer a natural formulation of the relation between bulk and boundary. In [13], an explicit isometry was constructed which maps the Hamiltonian $H_b$ onto another one $\tilde{H}_b$ acting on the space of auxiliary spins living at the edge of region A, while keeping the spectrum. Furthermore, for various two-dimensional (2D) models displaying quantum phase transitions, like a deformed AKLT [14] or an Ising-type [15] model, it was found [13] that a gapped bulk phase with local order corresponds to a boundary Hamiltonian with local interactions, whereas critical behavior in the bulk is reflected on a diverging interaction length of $\tilde{H}_b$.

Entanglement properties of 2D topological phases are less well understood. Rokhsar-Kivelson (RK) wave functions, defined as equal-weight superposition of fully packed dimer coverings, exhibit critical behavior on bipartite lattices [16] or realize the simplest topological phase, the so-called $\mathbb{Z}_2$ liquid, on frustrated lattices. [17] The topological EE of critical and topological RK wavefunctions have been computed using various topologies [18] and the boundary Hamiltonian corresponding to the GS of Kitaev's toric code [3] was shown to be *non-local.* [13] Unfortunately, RK-like wavefunctions are not generic – their ES is completely dispersionless [19] – and do not describe real quantum $S = 1/2$ spin systems. [20, 21] In contrast, (short-range) RVB states, defined as linear superposition of hardcore coverings of *non-orthogonal* nearest-neighbor *SU(2) singlets* (see Fig. 1(a)), appear to be closer to physical systems. Very recently, the (Renyi) EE between (finite) cylindrical regions has been computed [22] numerically for the critical [23, 24] RVB state on the square lattice. Similarly, the (Renyi) topological EE of SU(2)-symmetric gapped chiral and $\mathbb{Z}_2$ spin liquids was obtained [25] using Kitaev-Preskill prescription. Neverthe-

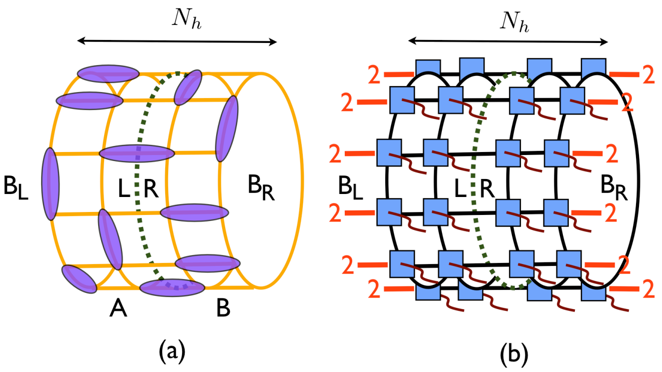

FIG. 1: (Color online) (a) Particular dimer hardcore covering on a $N_h \times N_v$ cylinder. Ellipses represent singlets of two spins 1/2. The RVB wavefunction is defined as the equal-weight superposition of all such configurations. Bi-partitioning the cylinder defines two (virtual) "L" and "R" edges. (b) PEPS on the same cylinder involving identical (rank-5) tensors (blue squares) on the sites with four virtual indices ($D = 3$) and one physical variable (curly line). The "B$_L$" and "B$_R$" boundaries are defined by the choice of the external indices (OBC correspond to choose "2" for all). Here, we take the limit $N_h \to \infty$ (infinitely long cylinder).

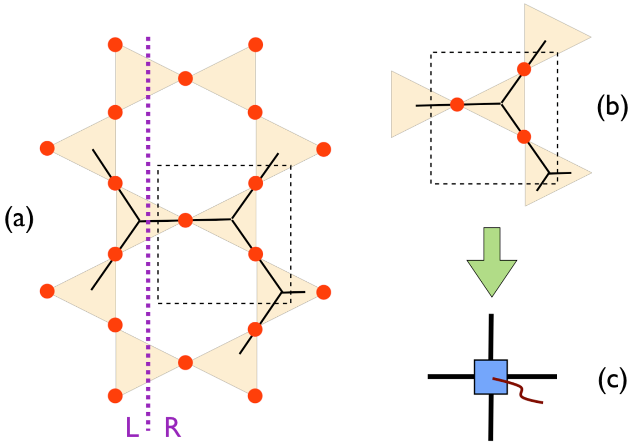

FIG. 2: (Color online) (a) Kagome lattice. The L and R edges are shown (thick dotted line). Three site tensors (red dots) carrying the physical indices and two 120-degree tensors (in the center of the shaded triangles) are grouped together (a,b) to construct the basic tensor (c).

less, ES and boundary Hamiltonians of such RVB/spin liquids wavefunctions is unknown. In this Letter, we study entanglement properties of both critical (square lattice) and gapped topologically-ordered (kagome lattice) RVB wavefunctions [24] on *infinite* cylinders making use of simple PEPS representations. In particular, we show that the boundary Hamiltonian can be written as a product of a highly non-local projector, which depends fundamentally on the boundary conditions, by a local one-dimensional t–J model, which arises due to the symmetry properties of the auxiliary spins at the boundary and characterizes the (gapless or gapped) edge modes. This multiplicative structure, a consequence of the disconnected topological sectors in the space of dimer coverings of the lattice, reflects then the topological nature of the states.

*PEPS representation of RVB states.* – We start with the square lattice RVB wavefunction (NN $|\uparrow\downarrow\rangle - |\downarrow\uparrow\rangle$ singlets are all oriented from one sublattice to the other) on a cylinder of length $N_h$ and circumference $N_v$, depicted in Fig. 1(a), which can be expanded in the local $S_z$-basis, $|\Psi_{\rm RVB}\rangle = \sum_S c_S |s_1, s_2, \ldots, s_M\rangle$, where $s_n = 0, 1$ are qubits (representing the two $S_z = \pm 1/2$ spin components) on the $M = N_h N_v$ sites and $S = \{s_n\}$. Such a state can be represented by a $D = 3$ PEPS [15, 21] (up to local unitaries) where each lattice site is replaced by a rank-5 tensor $A^s_{\alpha,\alpha';\beta,\beta'}$ labeled by one physical index, $s = 0$ or 1, and by four virtual bond indices (varying from 0 to 2) along the horizontal $(\alpha, \alpha')$ and vertical $(\beta, \beta')$ directions. Physically, the absence of singlet on a bond is encoded by the virtual index being "2" on that bond. To enforce the hardcore dimer constraint, one takes $A^s_{\alpha,\alpha';\beta,\beta'} = 1$ whenever three virtual indices equal 2 and the fourth one equals $s$, and $A^s_{\alpha,\alpha';\beta,\beta'} = 0$ otherwise. The amplitudes $c_S$ are then obtained by contracting all virtual indices, except the ones at the ends of the cylinder fixed by boundary conditions (BC), as depicted in Fig. 1(b). For the kagome lattice, as shown in Fig. 2, the RVB state can be represented in terms of rank-3 tensors, (i) $A^s_{\alpha;\beta}$ on the sites – $A^s_{2;s} = A^s_{s;2} = 1$ and zero otherwise – and (ii) on the center of each triangle, $R_{2,2,2} = 1$, and $R_{\alpha,\beta,\gamma} = \epsilon_{\alpha\beta\gamma}$ otherwise, with $\epsilon_{\alpha\beta\gamma}$ the antisymmetric tensor. [21] One can then group the 3 sites on each unit cell to obtain a rank-5 tensor (the physical dimension is now $2^3 = 8$) connected on an effective square lattice (Fig. 2(b,c)). Note that for the Kagome PEPS, one can find a local parent Hamiltonian for which the degeneracy is equal to 4 on the torus. [21]

*RDM on infinite cylinders* – The boundary Hamiltonian $\tilde{H}_b$ can be derived from the reduced density operator $\sigma_b^2 = \exp(-\tilde{H}_b)$ acting on the edge indices, following the procedure given in [13]. For the kagome lattice, there is no reflection symmetry w.r.t. the cut so the RDM for the left (right) side takes the form $\sigma^2_{bR} = \sqrt{\sigma_R^t}\sigma_L\sqrt{\sigma_R^t}$ ($\sigma^2_{bL} = \sqrt{\sigma_L^t}\sigma_R\sqrt{\sigma_L^t}$) where $\sigma_L$ and $\sigma_R$ are obtained by contracting the tensors of the left and right half-cylinders, respectively. [13] Note that $\sigma^2_{bL}$ and $\sigma^2_{bR}$ give identical ES. Here we are interested in RVB cylinders with infinite lengths in both directions. First, we fix the cylinder perimeter ($N_v = 4, 6, 8$) and take the limit $N_h \to \infty$ (in practice, the RDM for $N_h = 50$ is fully converged).

*Disconnected sectors* – A crucial feature of topological states is that the RDM depends intrinsically on the

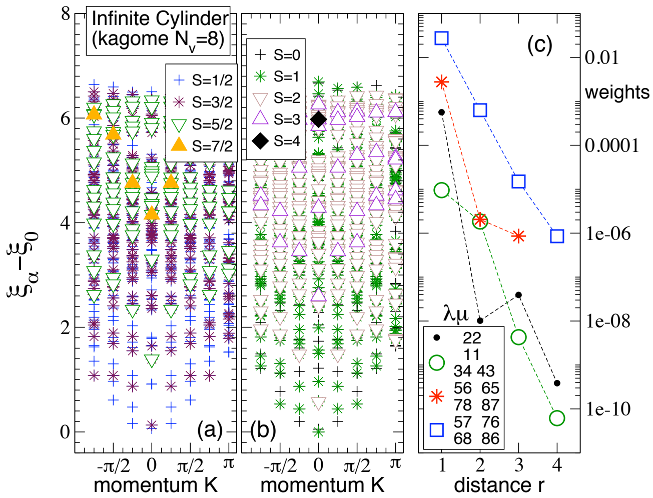

FIG. 3: (Color online) ES (w.r.t. the GS energy $\xi_0$) of an infinitely long kagome cylinder of perimeter $N_v = 8$. Eigenstates with half-integer (a) and integer (b) spins correspond to odd and even sectors, respectively (see text). (c) Weights $|d_{\lambda\mu}(r)|^2$ of the 2-body operators appearing in $H_{\rm local}$.

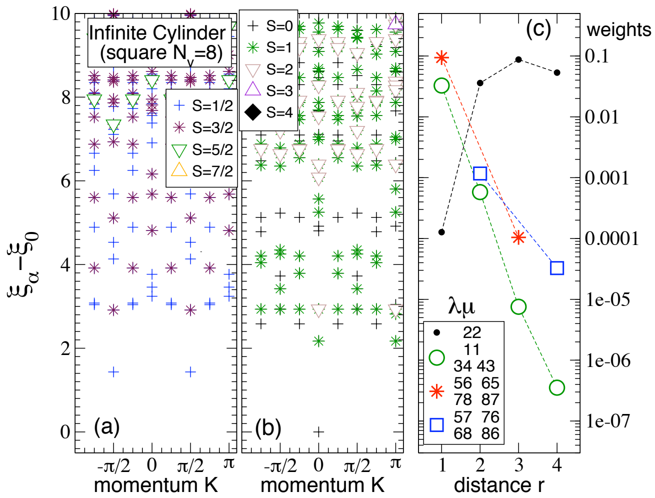

FIG. 4: (Color online) Same as Fig. 3 for the critical RVB state (square lattice). Eigenstates with half-integer (integer) spins correspond to $\Delta$ odd (even) – see text. For OBC one gets a subset of (b) ($\Delta = 0$ sector). (c) Weights $|d_{\lambda\mu}(r)|^2$ of the 2-body operators appearing in $H_{\rm local}$. The diagonal interaction $\hat{x}_2^i\hat{x}_2^{i+r}$ shows a long-range behavior.

choice of the BC ($B_L = B_R$ for simplicity), *even when* $N_h \to \infty$. Indeed, due to local constraints, (vertical) configurations of virtual indices can be grouped in disjoined conserved sectors which can be addressed independently from proper choices of $B_L = B_R$. Hence, although the RDM (and $\tilde{H}_b$) acts on all $3^{N_v}$ degrees of freedom of the $L$ (or $R$) edge, in each sector it contains a finite fraction of zero-weight eigenvalues, i.e. a finite fraction of eigenstates of $\tilde{H}_b$ have infinite-energy. Calling $\mathcal{P}$ the projector on the finite-energy subspace, we split $\tilde{H}_b$ as $\tilde{H}_b = H_1 + \beta_{\rm topo}(\mathrm{Id} - \mathcal{P})$, where Id is the $3^{N_v} \times 3^{N_v}$ identity-operator, $\beta_{\rm topo} \to \infty$, and $H_1$ is supported by the non-zero eigenvalues sector of the RDM. More precisely, $H_1$ can be factorized as $H_1 = H_{\rm local}\mathcal{P}$ where $H_{\rm local}$ is a Hamiltonian (shown later to be local) acting on the whole boundary space [28], commuting with $\mathcal{P}$ and *independent on BC*. The Kagome cylinder has only two sectors defined by $\mathcal{P} = \mathcal{P}_{\rm even}$ and $\mathcal{P} = \mathcal{P}_{\rm odd} = \mathrm{Id} - P_{\rm even}$, which can be obtained by choosing an even or odd number of "2" external (virtual) indices for $B_L = B_R$, respectively. For the RVB wavefunction on the square lattice, there are $N_v + 1$ disconnected sectors defined by projectors $\mathcal{P}_\Delta$ enforcing a fixed difference $N_{2,X} - N_{2,Y} = \Delta$ of the numbers of "2" on two X and Y alternating sublattices on the edge, $\Delta = -N_v/2, \cdots, N_v/2$. The fact that $H_1$ is known for all sectors implies that $H_{\rm local}$ is uniquely determined. [29] Open BC (OBC), relevant for physical systems, are defined by having "2" set on all the $B_L$ and $B_R$ indices (Fig. 1(b)). Therefore OBC give access to the even ($\Delta = 0$) sector on the kagome (square lattice) cylinder. [30]

*Bipartite entanglement spectrum* – The full ES is given by the spectrum of $H_{\rm local}$. Our results are summarized in Figs. 3(a,b) and 4(a,b), for infinitely-long cylinders with kagome and square lattices. The (excitation) ES are shown as a function of momentum around the cylinder and the eigenstates are labelled according to their spin-multiplet structure inherited from the su(2) symmetry of the RVB state, although with the $1/2 \oplus 0$ representation. [26] A careful finite size scaling suggests that the kagome (square) lattice cylinder ES is gapless (gapped) in the limit $N_v \to \infty$. Since these features are opposite to what is expected in the corresponding bulk systems, we deduce that the ES characterizes specifically the nature of the L and R edge modes (Fig. 1). Note that for given choice of BC, the actual ES is the spectrum of a *projected* $H_1$ Hamiltonian and, hence, is a subset of the full ES.

*Boundary Hamiltonian and non-locality* – Next, we investigate the exact connection between the boundary Hamiltonian and the bulk and *topological* properties of the system. We look for its explicit form, trying to make the connection with $D = 3$ models, with su(2) symmetry corresponding to the $1/2 \oplus 0$ representation. Any operator $\mathcal{O}_{\rm edge}$ acting on the edge can be expanded in terms of $3^{2N_v}$ orthogonal operators. For this purpose, we use a local basis of 9 (normalized) operators $\{\hat{x}_0, \cdots, \hat{x}_8\}$ which act on the local basis of configuration (at some site $i$), $\{|0\rangle, |1\rangle, |2\rangle\}$, e.g. $\hat{x}_0 = \mathbf{1}$, $\hat{x}_1 = \sqrt{\frac{3}{2}}(|0\rangle\langle 0| - |1\rangle\langle 1|)$ and $\hat{x}_2 = \frac{1}{\sqrt{2}}(|0\rangle\langle 0| + |1\rangle\langle 1| - 2|2\rangle\langle 2|)$, for the diagonal matrices, complemented by $\hat{x}_3 = \hat{x}_4^\dagger = \sqrt{3}|0\rangle\langle 1|$ acting as "spin" operators, and $\hat{x}_5 = \hat{x}_7^\dagger = \sqrt{3}|2\rangle\langle 0|$

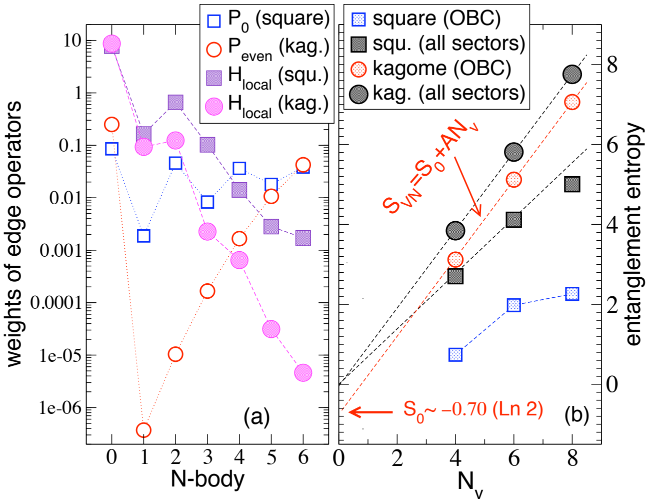

FIG. 5: (Color online) (a) Distribution of weights vs N (semi-log plot) of $\mathcal{P}_{\rm even}$, $\mathcal{P}_0$ – corresponding to OBC – and of $H_{\rm local}$ for kagome (circles) and square (squares) lattices ($N_v = 8$). (b) Entanglement entropy versus $N_v$ for OBC (open symbols) or when summing over all sectors (shaded symbols).

and $\hat{x}_6 = \hat{x}_8^\dagger = \sqrt{3}|2\rangle\langle 1|$ acting as annihilation and creation (hardcore) bosonic operators. [27] The expansion in terms of N-body operators reads,

$$\begin{aligned}\mathcal{O}_{\rm edge} &= c_0 N_v + \sum_{\lambda,i} c_\lambda \hat{x}_\lambda^i + \sum_{\lambda,\mu,r,i} d_{\lambda\mu}(r)\, \hat{x}_\lambda^i \hat{x}_\mu^{i+r} \\ &+ \sum_{\lambda,\mu,\nu,r,r',i} e_{\lambda\mu\nu}(r,r')\, \hat{x}_\lambda^i \hat{x}_\mu^{i+r} \hat{x}_\nu^{i+r'} + \cdots, \quad (1)\end{aligned}$$

where each group of terms involves products of $N$ ($1 \leq N \leq N_v$) on-site $\hat{x}_\lambda$ ($\lambda \neq 0$) operators. Here the sums are restricted to non-equivalent relative distances and only translations giving *distinct* sets of sites are performed. As seen from the distribution of their weights in Fig. 5(a), projectors are highly non-local, conferring a fundamentally non-local character to the boundary Hamiltonian $H_1$. This is also to be expected for *realistic* topological GS of microscopic Hamiltonians on geometries involving open or fixed BC in some directions. In contrast, $H_{\rm local}$ [29] contains primarily one- and two-body contributions (Fig. 5(a)). The weights of all (non-zero) two–body terms of $H_{\rm local}$ shown in Figs. 3(c),4(c) reveal exponential decays with distance $r$, except for a diagonal term in the case of the square lattice. These remarkable features are to be connected to the bulk correlations of the RVB wavefunctions, short-range in the kagome lattice and critical for the square lattice. Interestingly, $H_{\rm local}$ is formally equivalent to a one-dimensional "t–J model" [31] describing motion of "holes" (the "2") in a spin fluctuating background (the '0" and "1" qbits) supplemented by additional density-density and pair-field terms, conferring a superfluid character to the edge.

*Topological entropy.* – For infinite cylinders of the kagome lattice with OBC, the EE $S_{VN} = -{\rm Tr}\{\sigma_b^2 \ln \sigma_b^2\}$ can be well fitted according to $S_{VN} = S_0 + AN_v$, as shown in Fig. 5(b), where $S_0$ is the topological EE. The existence of a finite $S_0$ is a direct consequence of the particular structure of $H_1$. Indeed, the EE is given (crudely) by $-\ln \mathcal{N}$ where $\mathcal{N}$ is the number of eigenstates of $H_1$ below a fixed energy scale of order 1. For OBC, the support of $H_1 = H_{\rm local}\mathcal{P}_{\rm even}$ contains $\mathcal{N} \simeq \frac{1}{2}3^{Nv}$ states and $S_0 = -\ln 2$, as expected for a topological $\mathbb{Z}_2$ spin liquid. Summing over all sectors amounts to take $H_1 = H_{\rm local}$ so that all eigenstates of the ES contribute and $S_{VN} \propto N_v$ (as can be shown rigorously) as seen in Fig. 5(b). For the square lattice, severe constraints leads to an *extensive* number (i.e. proportional to the perimeter $N_v$) of disconnected sectors on the edge of dimension $\mathcal{N} \simeq \frac{1}{N_v} 3^{N v}$, therefore introducing *negative* logarithmic corrections $\sim -\ln N_v$ to the EE for any BC (see e.g. data for OBC on Fig. 5(b)). The long-range diagonal interaction in $H_{\rm local}$ (Fig. 4(c)) is also responsible for deviations from the area law, even when considering all sectors.

*Discussion and outlook.* – We have shown that boundary Hamiltonians associated to gapped and gapless RVB states can be written as $H_{\rm local}\mathcal{P} + \beta_{\rm topo}({\rm Id} - \mathcal{P})$, $\beta_{\rm topo} \to \infty$. In particular, we have established the existence of a projector $\mathcal{P}$ (which intrinsically depends on the BC) onto a restricted subspace at the edge (as for Kitaev toric code [3, 13]), a consequence of the disconnected topological sectors in the space of dimer coverings of the lattice. We argue that the non-local character of the resulting boundary Hamiltonian is the fingerprint of topology. The ES is a subset (associated to $\mathcal{P}$) of the spectrum of the emerging local Hamiltonian $H_{\rm local}$ acting on the unrestricted edge space. In contrast to the toric code for which $H_{\rm local}$ is trivial, here $H_{\rm local}$ takes the form of a short-range (bosonic) t–J model (including a long-range diagonal interaction for the critical RVB state). We propose to use the features of the boundary Hamiltonian to detect topological phases in microscopic models. [6–8]

D.P. acknowledges support by the "Agence Nationale de la Recherche" under grant No. ANR 2010 BLANC 0406-0. This work was granted access to the HPC resources of CALMIP under the allocation 2012-P1231. N.S. acknowledges helpful discussions with Frank Verstraete and support by the Alexander von Humboldt foundation, the Institute for Quantum Information and Matter (an NSF Physics Frontiers Center with support of the Gordon and Betty Moore Foundation) and the NSF Grant No. PHY-0803371. D.P.-G. acknowledges QUEVADIS and Spanish grants QUITEMAD and MTM2011-26912. J.I.C. acknowledges the EC project Quevadis, the DFG Forschergruppe 635, and Caixa Manresa. This work was initiated at Centro de Ciencias Pedro Pascual (Benasque, Spain).

---

[1] X. G. Wen, *Int. J. Mod. Phys.* B **5**, 1641 (1991).

[2] P. W. Anderson, *Mater. Res. Bull.* **8**, 153 (1973); P. Fazekas and P. W. Anderson, *Philos. Mag.* **30**, 432 (1974).

[3] A. Kitaev, *Ann. Phys.* **303**, 2 (2003); quant-ph/9707021.

[4] P. Mendels et al., Phys. Rev. Lett. **98**, 077204 (2007) and references therein.

[5] G. Misguich and C. Lhuillier, "Two-dimensional quantum antiferromagnet", in "Frustrated spin systems", edited by H. T. Diep editor, World-Scientific (2005).

[6] Z. Y. Meng, T. C. Lang, S. Wessel, F. F. Assaad, and A. Muramatsu, Nature **464**, 847 (2010); B. K. Clark, D. A. Abanin, and S. L. Sondhi, Phys. Rev. Lett. **107**, 087204 (2011).

[7] Simeng Yan, David A. Huse and Steven R. White, Science **332**, 1173 (2011).

[8] Hong-Chen Jiang, Hong Yao, Leon Balents, arXiv:1112.2241.

[9] A. Kitaev and J. Preskill, *Phys. Rev. Lett.* **96**, 110404 (2006); M. Levin and X.-G. Wen, *Phys. Rev. Lett.* **96**, 110405 (2006).

[10] H. Li and F. D. M Haldane, *Phys. Rev. Lett.* **101**, 010504 (2008); R. Thomale, A. Sterdyniak, N. Regnault, and B. A. Bernevig, *Phys. Rev. Lett.* **104**, 180502 (2010).

[11] D. Poilblanc, *Phys. Rev. Lett.* **105**, 077202 (2010); see also R. Thomale, D. P. Arovas, and B. A. Bernevig, *Phys. Rev. Lett.* **105**, 116805 (2010), using a "momentum cut".

[12] F. Verstraete and J. I. Cirac, arXiv:cond-mat/0407066; F. Verstraete and J. I. Cirac, *Phys. Rev. A* **70**, 060302(R) (2004); J. I. Cirac and F. Verstraete, *J. Phys. A: Math. Theor.* **42**, 504004 (2009).

[13] J. I. Cirac, D. Poilblanc, N. Schuch, and F. Verstraete, *Phys. Rev. B* **83**, 245134 (2011).

[14] I. Affleck, T. Kennedy, E. H. Lieb and H. Tasaki, *Phys. Rev. Lett.* **59**, 799 (1987); *ibid*, *Commun. Math. Phys.* **115**, 477 (1988).

[15] F. Verstraete, M. M. Wolf, D. Perez-Garcia and J. I. Cirac, *Phys. Rev. Lett.* **96**, 220601 (2006).

[16] D. S. Rokhsar and S. A. Kivelson, *Phys. Rev. Lett.* **61**, 2376 (1988).

[17] R. Moessner and S. Sondhi, *Phys. Rev. Lett.* **86**, 1881 (2001); G. Misguich, D. Serban, and V. Pasquier, *Phys. Rev. Lett.* **89**, 137202 (2002).

[18] S.. Furukawa and G. Misguich, *Phys. Rev. B* **75**, 214407 (2007); S. T. Flammia, A. Hamma, T. L. Hughes, and X.-G. Wen, *Phys. Rev. Lett.* **103**, 261601 (2009); J.-M. Stephan, S. Furukawa, G. Misguich, and V. Pasquier, *Phys. Rev. B* **80**, 184421 (2009). For Kitaev's toric code, see Hong Yao and Xiao-Liang Qi, *Phys. Rev. Lett.* **105**, 080501 (2010).

[19] J.-M. Stephan, G. Misguich, and V. Pasquier, J. Stat. Mech. P02003 (2012).

[20] Nevertheless, a dimer wavefunction on the Kagome lattice can be mapped to Kitaev's toric code on the square lattice, which indicates that in the former case there should exist a non-local boundary Hamiltonian. [21]

[21] N. Schuch, D. Poilblanc, J. I. Cirac, and D. Pérez-García, arXiv:1203.4816.

[22] Hyejin Ju, A. B. Kallin, P. Fendley, M. B. Hastings, and R. G. Melko, arXiv:1112.4474v1.

[23] A. F. Albuquerque and F. Alet, Phys. Rev. B **82**, 180408 (2010).

[24] The critical or short-range behavior of the RVB wavefunctions can also be inferred from finite size analysis of the correlation lengths obtained from the PEPS transfer matrices.

[25] Y. Zhang, T. Grover, and A. Vishwanath, *Phys. Rev. B* **84**, 075128 (2011).

[26] D. Perez-Garcia et al., *New J. Phys.* **12**, 025010 (2010).

[27] The trivial action of local operators on the unspecified sites is left implicit. Formally, $\hat{x}_\lambda := \hat{x}_\lambda \otimes \mathbf{1}^{\otimes(N_v-1)}$.

[28] On the kagome lattice, $H_{\mathrm{local}}$ corresponding to the L and R edges differ slightly. Here, we refer to the L edge.

[29] By summing up over the sectors, the different projectors add up to the identity so one can get directly $H_{\mathrm{local}}$ from an appropriate average of the corresponding RDMs.

[30] The other sectors can be addressed physically by imposing a magnetic field on some spins of the boundaries so that they point up – this is like putting $|1\rangle$'s on $B_L$ and $B_R$.

[31] M. Ogata, M. U. Luchini, S. Sorella, and F. F. Assaad, *Phys. Rev. Lett.* **66**, 2388 (1991).